

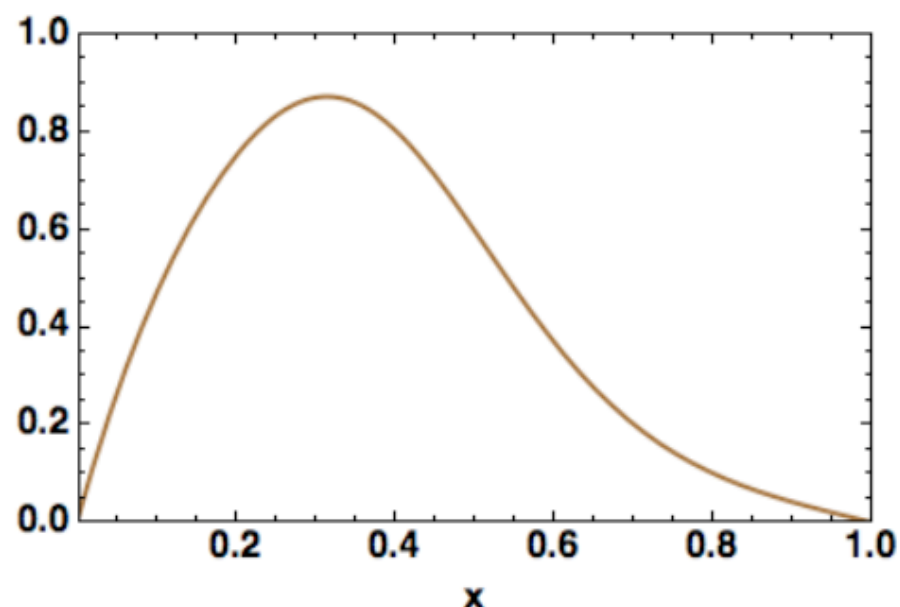


Semi-Inclusive π^0 target and beam-target asymmetries from 6 GeV electron scattering with CLAS

Keith Griffioen
William & Mary
for the EG1-DVCS Analysis Group
29 March 2017

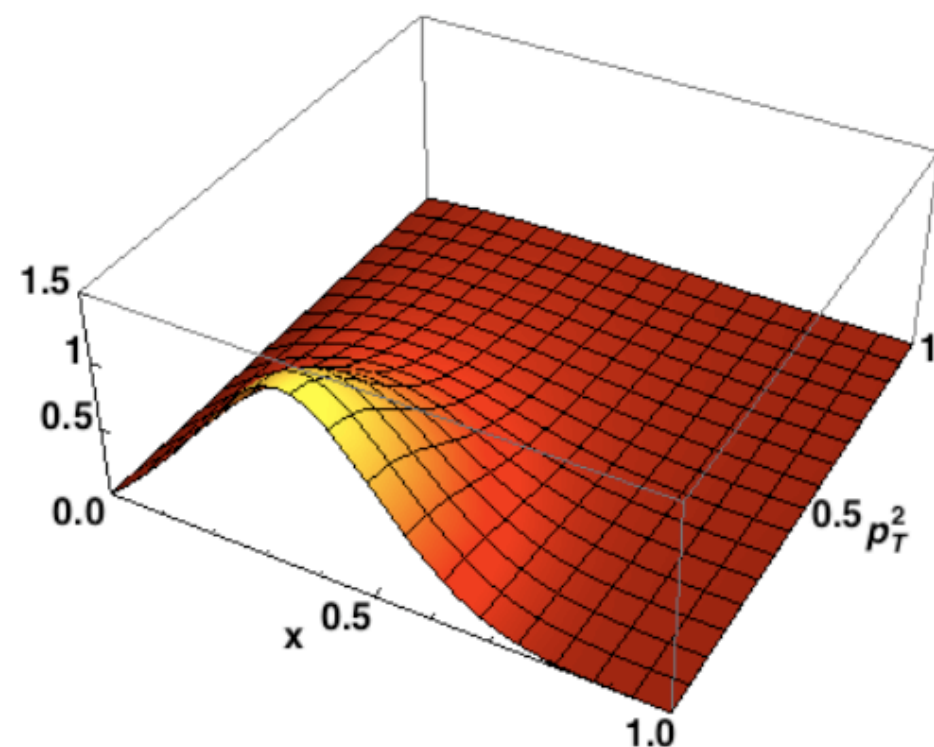
- Any confined quark must have transverse momentum
- Therefore, collinear PDFs cannot give the whole story
- Transverse momentum is related to L_z
- There has been much recent work trying to understand transverse momentum distributions (TMDs)

$$x f_1^u(x)$$

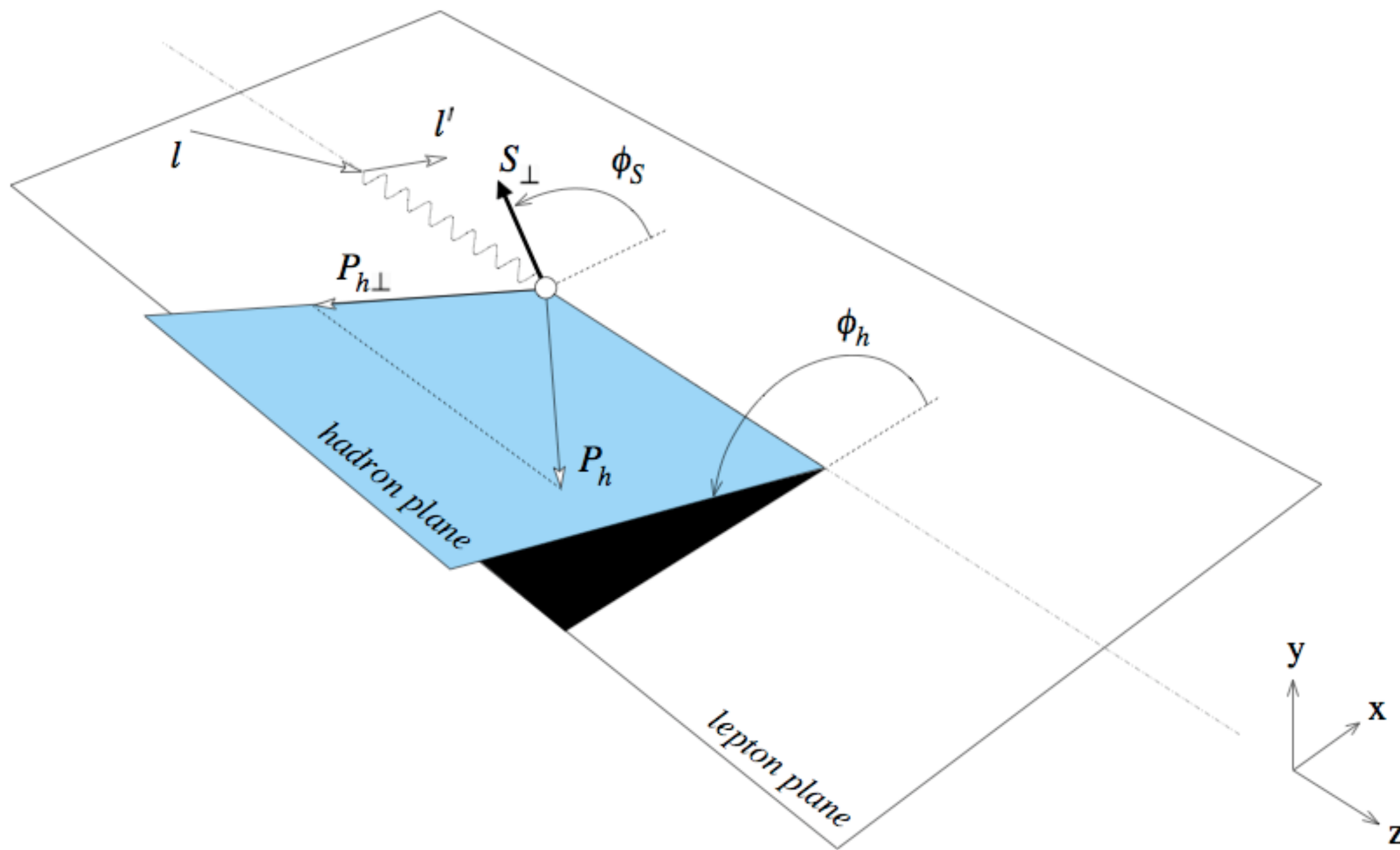


Standard collinear PDF

$$x f_1^u(x, p_T^2)$$



TMD



Bacchetta, et al., JHEP 2(2007)093

$$\begin{aligned}
 \frac{d\sigma}{dx dy d\psi dz d\phi_h dP_{h\perp}^2} = & \frac{\alpha^2}{xyQ^2} \frac{y^2}{2(1-\varepsilon)} \left(1 + \frac{\gamma^2}{2x}\right) \left\{ F_{UU,T} + \varepsilon F_{UU,L} + \sqrt{2\varepsilon(1+\varepsilon)} \cos\phi_h F_{UU}^{\cos\phi_h} \right. \\
 & + \varepsilon \cos(2\phi_h) F_{UU}^{\cos 2\phi_h} + \lambda_e \sqrt{2\varepsilon(1-\varepsilon)} \sin\phi_h F_{LU}^{\sin\phi_h} \\
 & + S_{\parallel} \left[\sqrt{2\varepsilon(1+\varepsilon)} \sin\phi_h F_{UL}^{\sin\phi_h} + \varepsilon \sin(2\phi_h) F_{UL}^{\sin 2\phi_h} \right] \\
 & + S_{\parallel} \lambda_e \left[\sqrt{1-\varepsilon^2} F_{LL} + \sqrt{2\varepsilon(1-\varepsilon)} \cos\phi_h F_{LL}^{\cos\phi_h} \right] \\
 & + |S_{\perp}| \left[\sin(\phi_h - \phi_S) \left(F_{UT,T}^{\sin(\phi_h - \phi_S)} + \varepsilon F_{UT,L}^{\sin(\phi_h - \phi_S)} \right) \right. \\
 & + \varepsilon \sin(\phi_h + \phi_S) F_{UT}^{\sin(\phi_h + \phi_S)} + \varepsilon \sin(3\phi_h - \phi_S) F_{UT}^{\sin(3\phi_h - \phi_S)} \\
 & + \left. \sqrt{2\varepsilon(1+\varepsilon)} \sin\phi_S F_{UT}^{\sin\phi_S} + \sqrt{2\varepsilon(1+\varepsilon)} \sin(2\phi_h - \phi_S) F_{UT}^{\sin(2\phi_h - \phi_S)} \right] \\
 & + |S_{\perp}| \lambda_e \left[\sqrt{1-\varepsilon^2} \cos(\phi_h - \phi_S) F_{LT}^{\cos(\phi_h - \phi_S)} + \sqrt{2\varepsilon(1-\varepsilon)} \cos\phi_S F_{LT}^{\cos\phi_S} \right. \\
 & + \left. \left. \sqrt{2\varepsilon(1-\varepsilon)} \cos(2\phi_h - \phi_S) F_{LT}^{\cos(2\phi_h - \phi_S)} \right] \right\},
 \end{aligned}$$



Leading Twist



Sub-Leading Twist
(extra factor of 1/Q)



0 (i.e. $R = \sigma_L / \sigma_T = 0$)

$A_{UL} = \{\text{UL terms}\} / \{\text{UU terms}\}$

$A_{LL} = \{\text{LL terms}\} / \{\text{UU terms}\}$

etc.

$$\mathcal{C}[w f D] = x \sum_a e_a^2 \int d^2 \mathbf{p}_T d^2 \mathbf{k}_T \delta^{(2)}(\mathbf{p}_T - \mathbf{k}_T - \mathbf{P}_{h\perp}/z) w(\mathbf{p}_T, \mathbf{k}_T) f^a(x, p_T^2) D^a(z, k_T^2)$$

$$F_{UU,T} = \mathcal{C}[f_1 D_1]$$

Unpolarized
fragmentation function;
integrates to $D_1(z, Q^2)$

$$F_{LL} = \mathcal{C}[g_{1L} D_1]$$

Unpolarized structure
function; integrates to
 $F_1(x, Q^2)$

$$F_{UT}^{\sin(\phi_h + \phi_S)} = \mathcal{C}\left[-\frac{\hat{\mathbf{h}} \cdot \mathbf{k}_T}{M_h} h_1 H_1^\perp\right]$$

Polarized structure
function; integrates to
 $g_1(x, Q^2)$

$$F_{UT,T}^{\sin(\phi_h - \phi_S)} = \mathcal{C}\left[-\frac{\hat{\mathbf{h}} \cdot \mathbf{p}_T}{M} f_{1T}^\perp D_1\right]$$

The Collins
fragmentation function

The Sivers structure
function

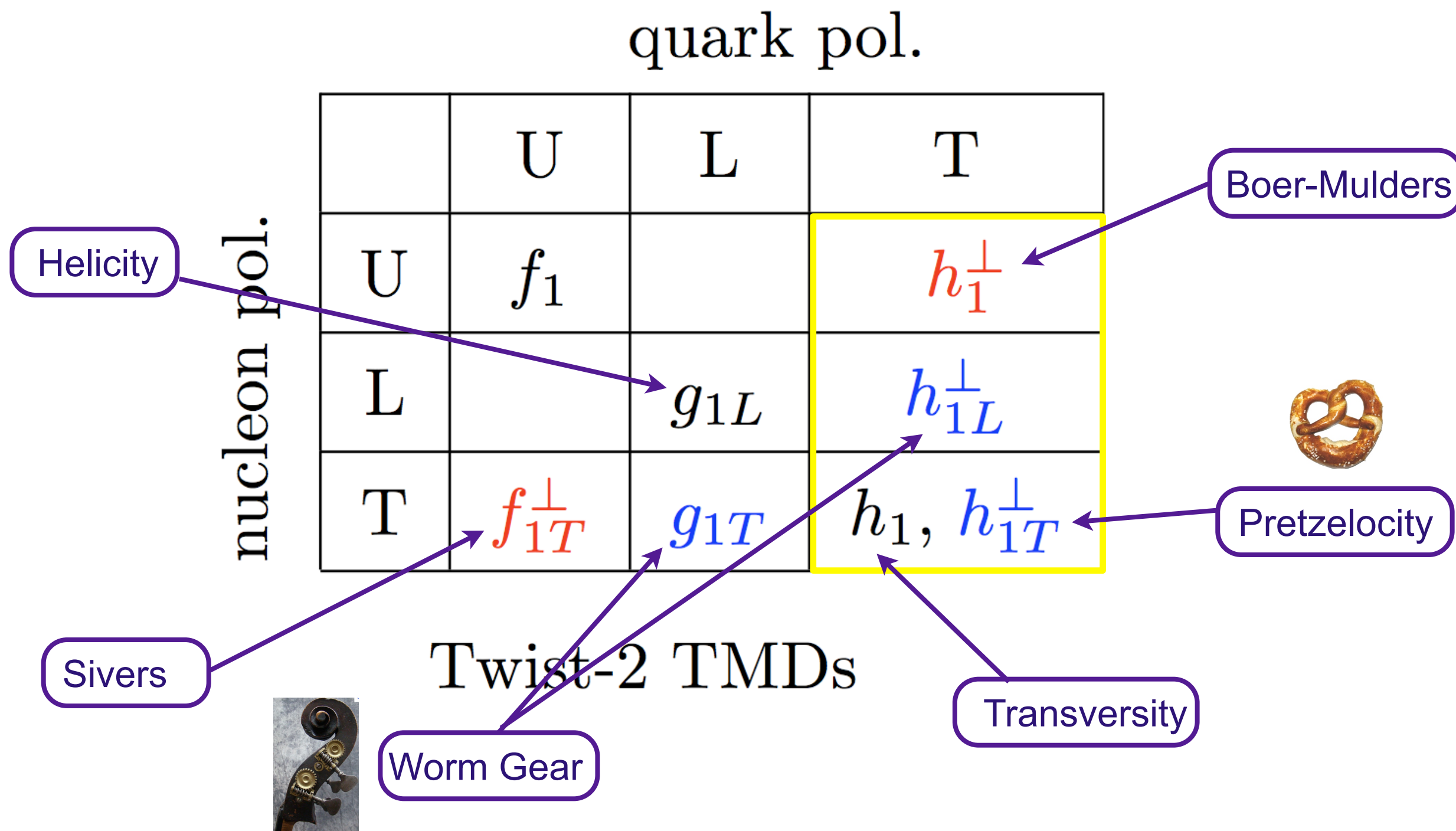
And there are more...



Red: T-odd

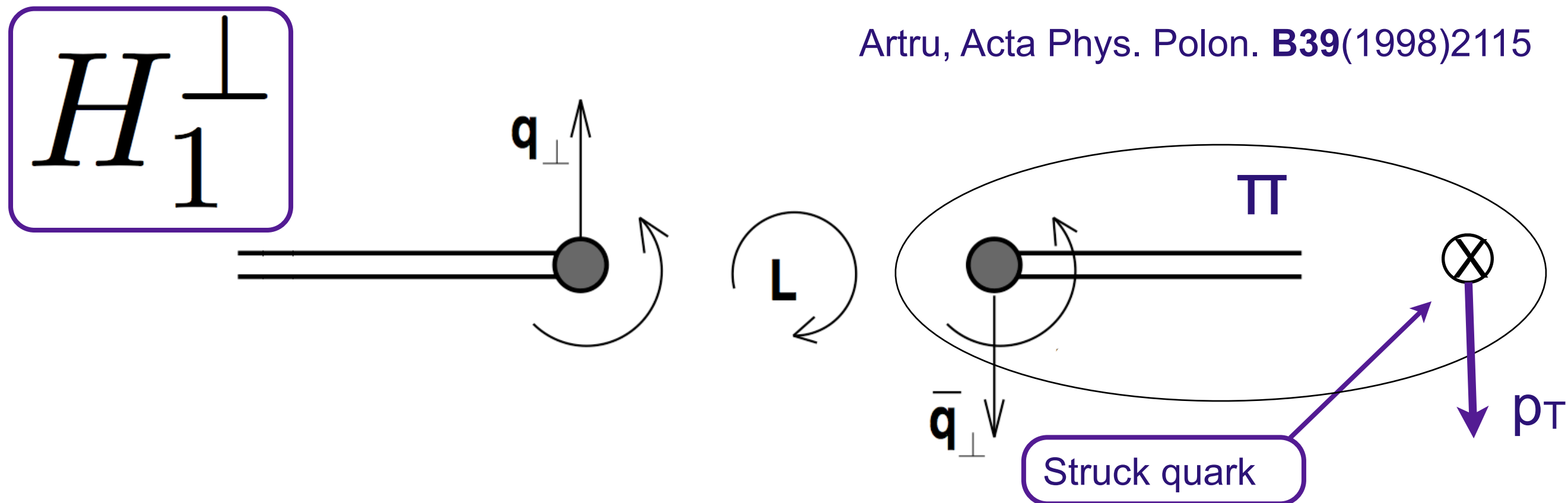
Black: survive p_T integration

Yellow box: chiral-odd



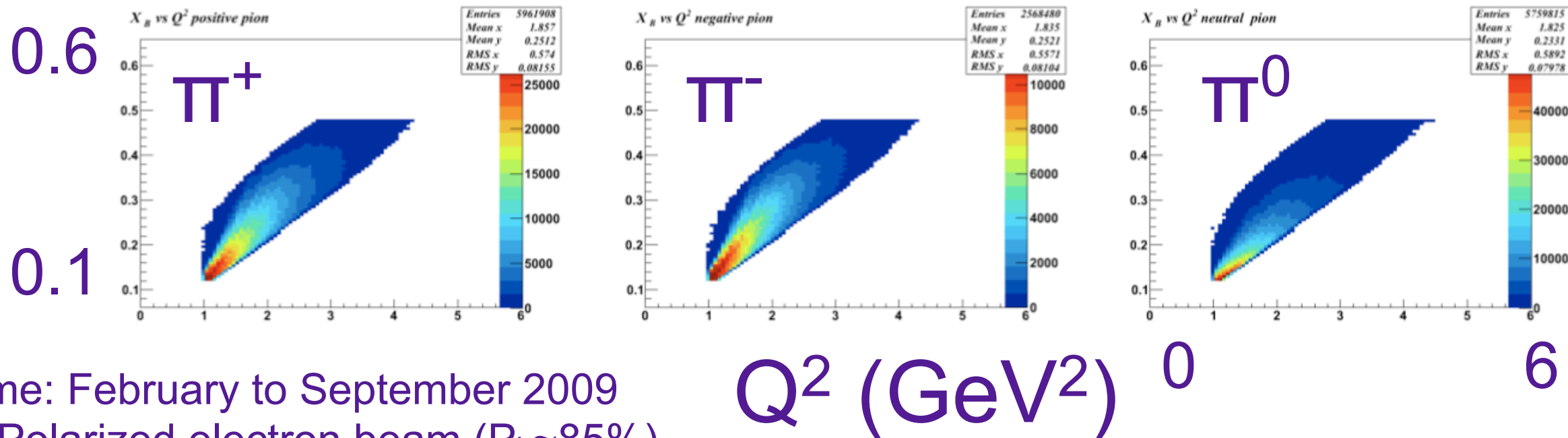
Collins Fragmentation

Artru, Acta Phys. Polon. **B39**(1998)2115



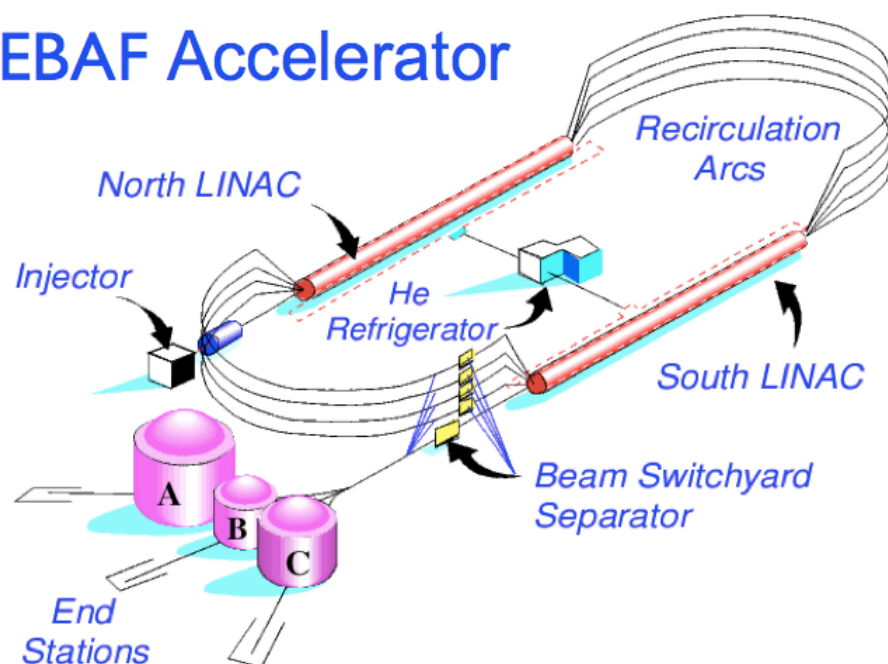
- Imagine that the $q\bar{q}$ pair is created in a 3P_0 spin state with vacuum quantum numbers $J^{PC}=0^{++}$
- Quark spins are opposite the orbital ang. mom. $L=1$
- Pion (with no spin) acquires transverse momentum
- This simple model breaks down if the fragmentation string does not conserve J (i.e. if there are torques)

X



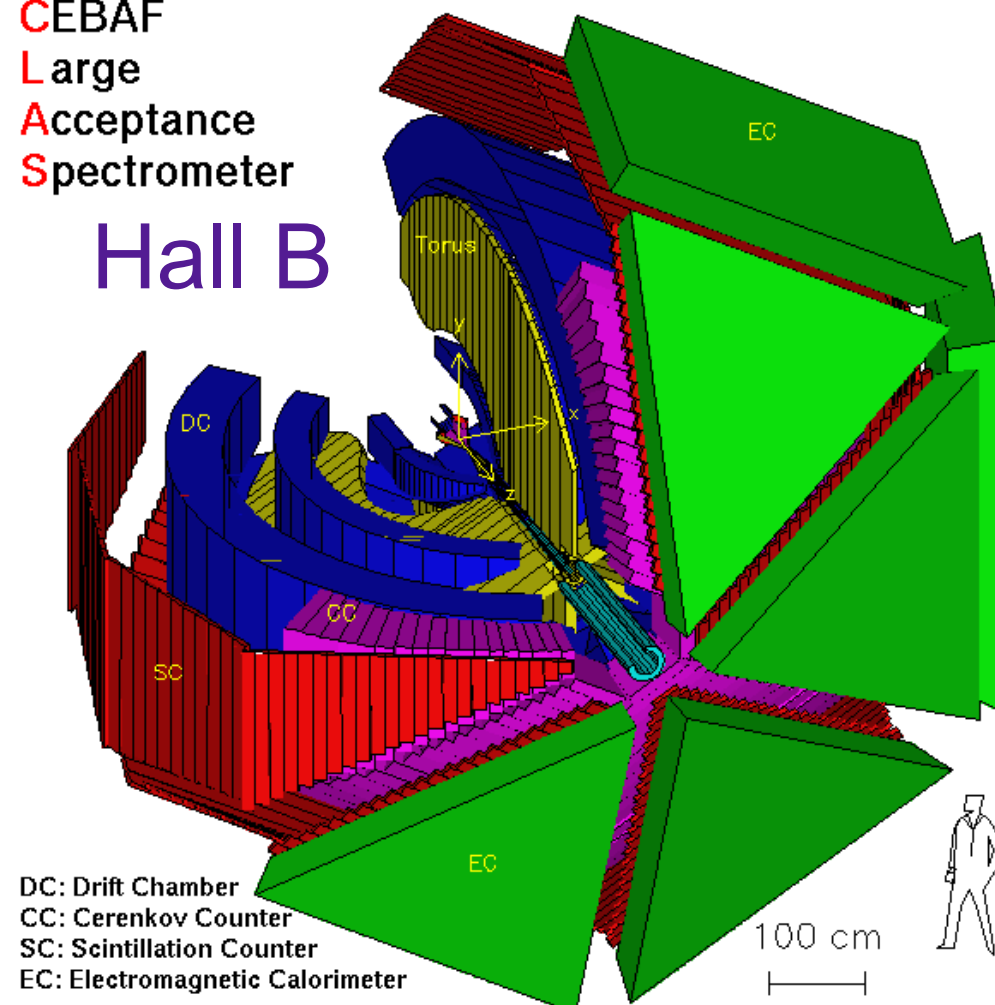
- Beam time: February to September 2009
- ~6 GeV Polarized electron beam ($P_b \sim 85\%$)
- Frozen $^{14}\text{NH}_3$ target ($P_t \sim 75\%$)
- CEBAF large acceptance spectrometer (CLAS) plus Inner Calorimeter
- ~19 billion electron triggers on NH_3 target

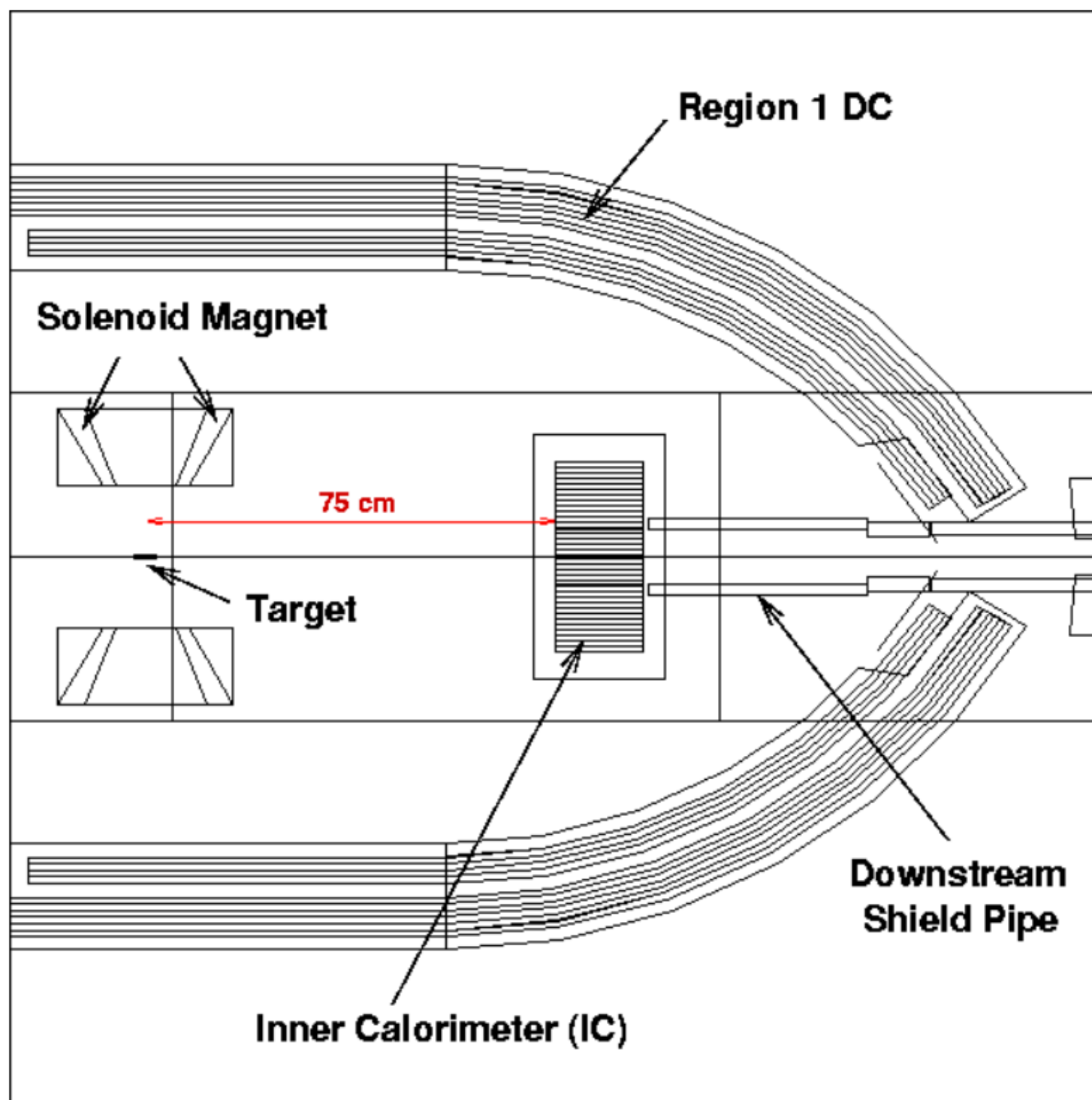
The CEBAF Accelerator



CEBAF
Large
Acceptance
Spectrometer

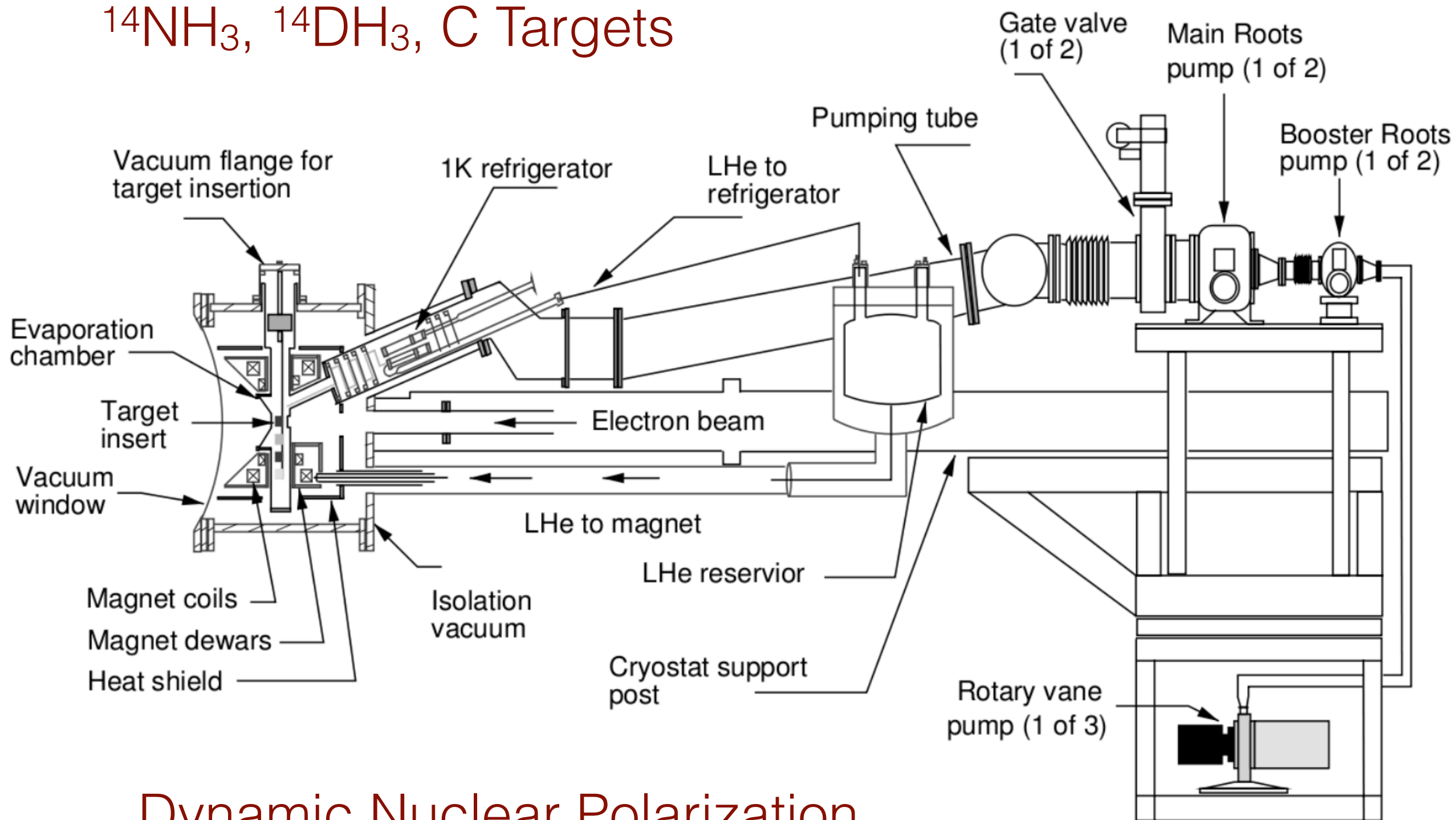
Hall B





$$\pi^0 \rightarrow \gamma\gamma$$

$^{14}\text{NH}_3$, $^{14}\text{DH}_3$, C Targets



Dynamic Nuclear Polarization

$$A_{LU} = \frac{(d\sigma^{\uparrow\uparrow} - d\sigma^{\downarrow\uparrow}) + (d\sigma^{\uparrow\downarrow} - d\sigma^{\downarrow\downarrow})}{(d\sigma^{\uparrow\uparrow} + d\sigma^{\downarrow\uparrow}) + (d\sigma^{\uparrow\downarrow} + d\sigma^{\downarrow\downarrow})},$$

$$A_{UL} = \frac{d\sigma^{\uparrow\uparrow} + d\sigma^{\downarrow\uparrow} - d\sigma^{\uparrow\downarrow} - d\sigma^{\downarrow\downarrow}}{(d\sigma^{\uparrow\uparrow} + d\sigma^{\downarrow\uparrow}) + (d\sigma^{\uparrow\downarrow} + d\sigma^{\downarrow\downarrow})},$$

$$A_{LL} = \frac{-d\sigma^{\uparrow\uparrow} + d\sigma^{\downarrow\uparrow} + d\sigma^{\uparrow\downarrow} - d\sigma^{\downarrow\downarrow}}{(d\sigma^{\uparrow\uparrow} + d\sigma^{\downarrow\uparrow}) + (d\sigma^{\uparrow\downarrow} + d\sigma^{\downarrow\downarrow})},$$

$$A_{LU} = \frac{A_{LU}^{\sin \phi_h} \sin \phi_h}{1 + A_{UU}^{\cos \phi_h} \cos \phi_h + A_{UU}^{\cos 2\phi_h} \cos 2\phi_h}$$

$$A_{UL} = \frac{A_{UL}^{\sin \phi_h} \sin \phi_h + A_{UL}^{\sin 2\phi_h} \sin 2\phi_h}{1 + A_{UU}^{\cos \phi_h} \cos \phi_h + A_{UU}^{\cos 2\phi_h} \cos 2\phi_h}$$

$$A_{LL} = \frac{A_{LL}^{Const} + A_{LL}^{\cos \phi_h} \cos \phi_h}{1 + A_{UU}^{\cos \phi_h} \cos \phi_h + A_{UU}^{\cos 2\phi_h} \cos 2\phi_h};$$

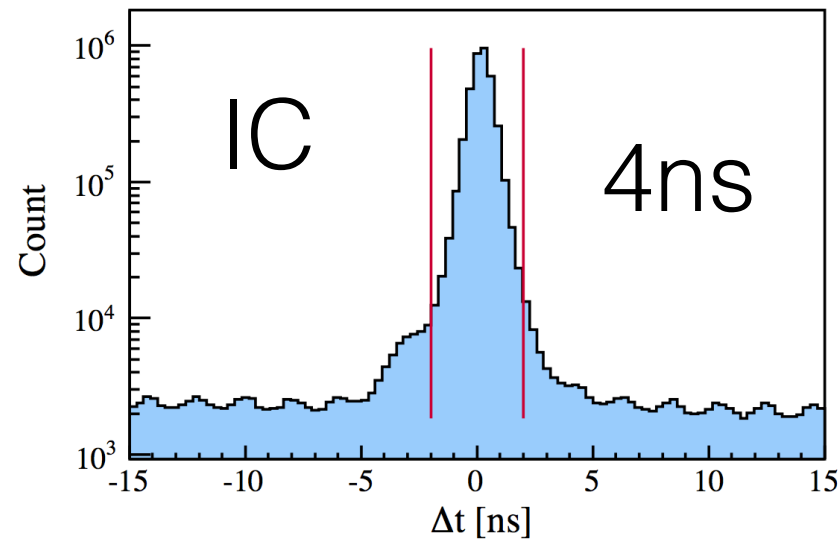


Figure 3.31: Δt distribution for IC photons after applying all other photon cuts. For a good IC photon candidate, Δt is required to be within ± 2 ns.

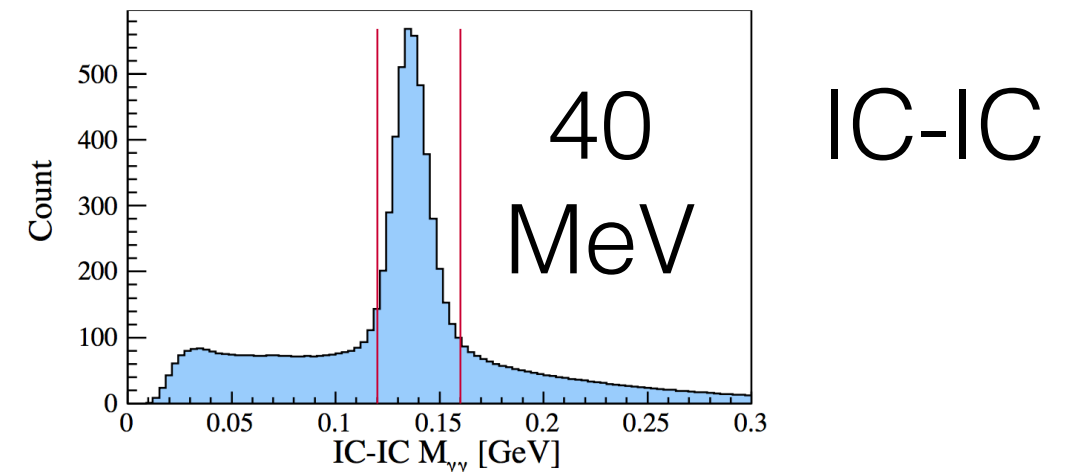


Figure 3.35: $M_{\gamma_{IC}-\gamma_{IC}}$. The invariant mass distribution of two photons, both in the IC. The vertical red lines represent the applied cuts, $0.12 \text{ GeV} \leq M_{\gamma_{IC}-\gamma_{IC}} \leq 0.16 \text{ GeV}$.

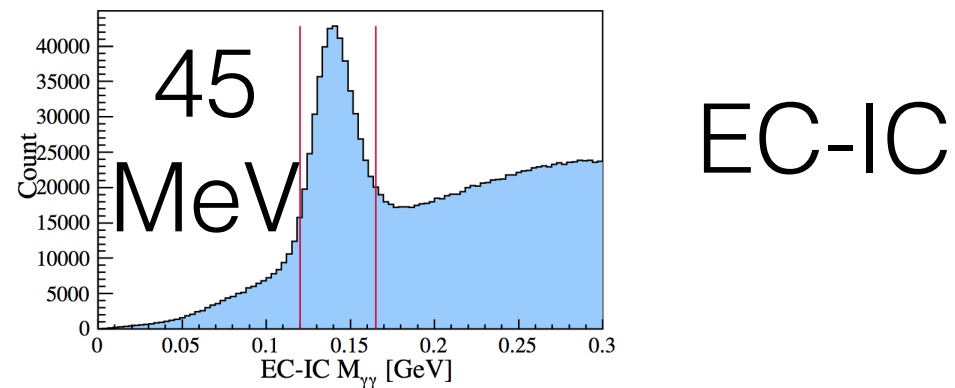


Figure 3.34: $M_{\gamma_{EC}-\gamma_{IC}}$. The invariant mass distribution of two photons, one in EC and one in IC. The vertical red lines represent the applied cuts, $0.12 \text{ GeV} \leq M_{\gamma_{EC}-\gamma_{IC}} \leq 0.165 \text{ GeV}$.

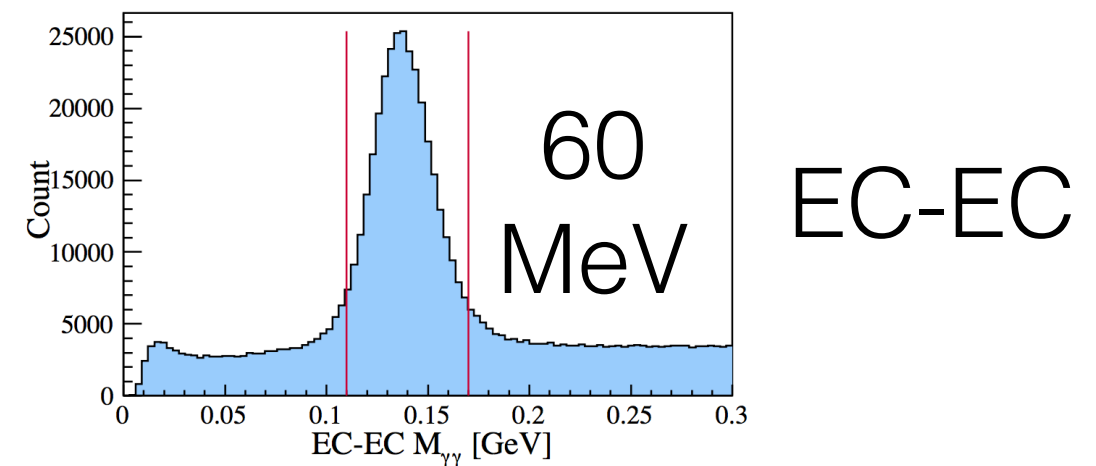
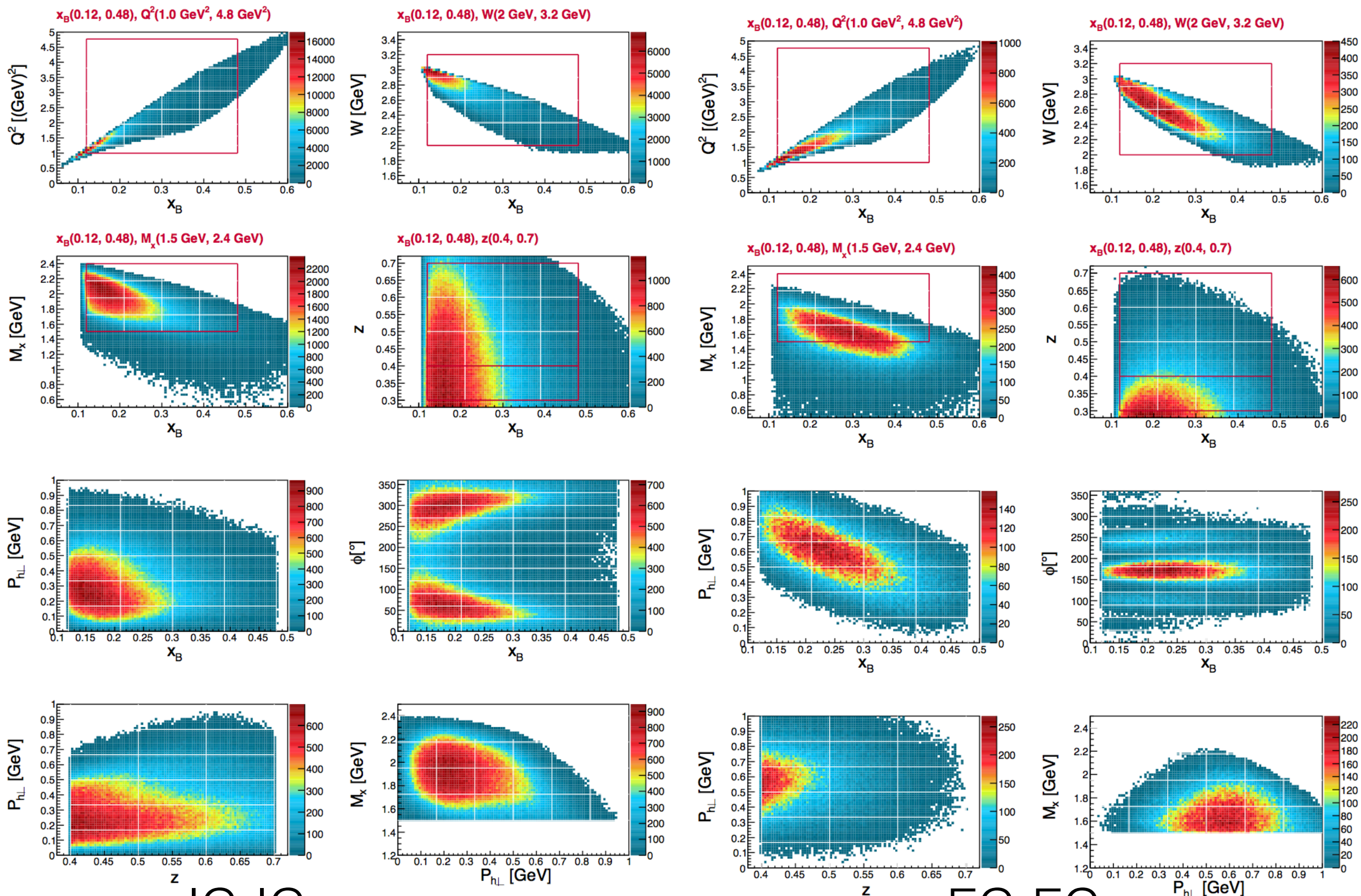


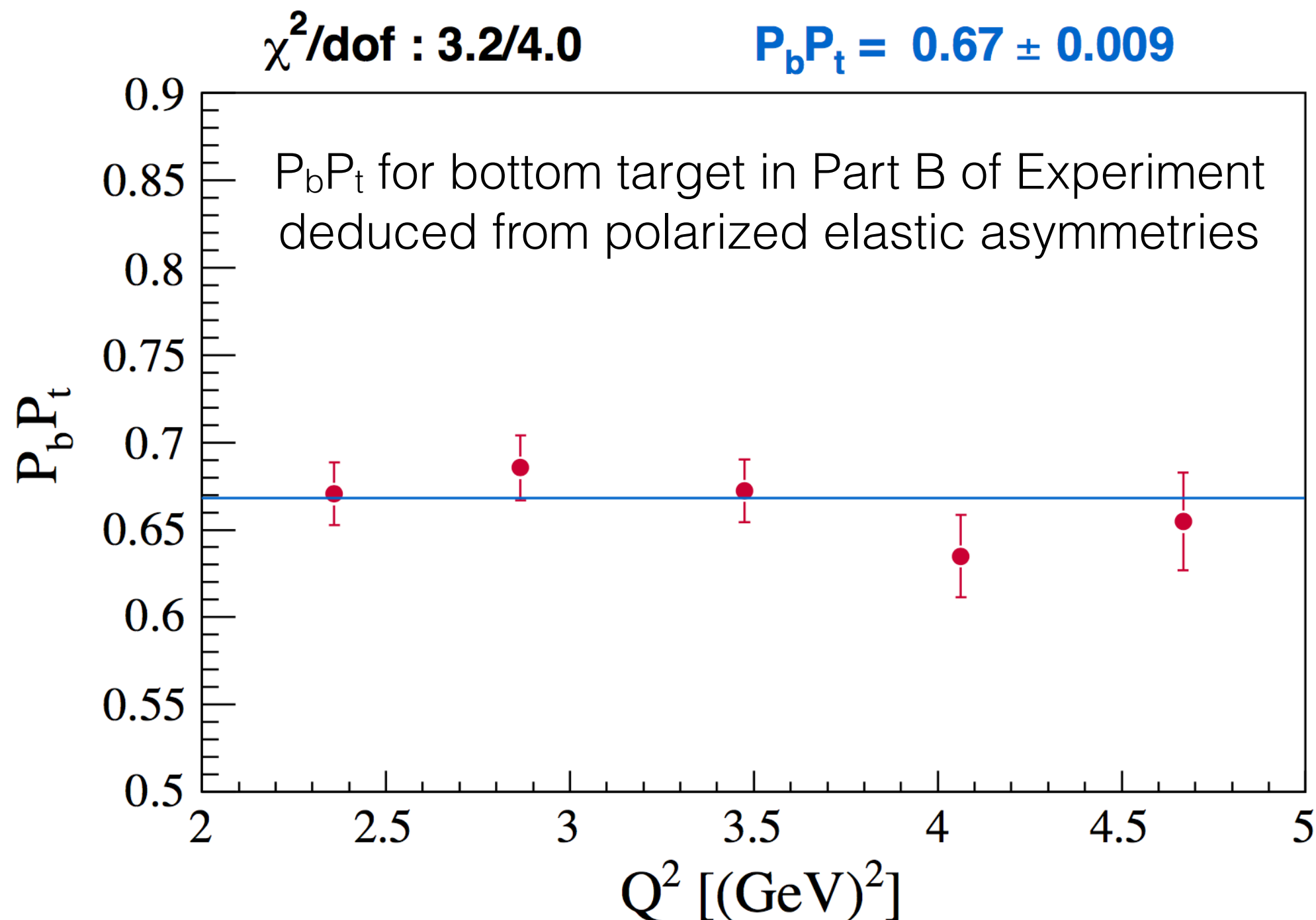
Figure 3.33: $M_{\gamma_{EC}-\gamma_{EC}}$. The invariant mass distribution of two photons, both in the EC. The vertical red lines represent the applied cuts, $0.11 \text{ GeV} \leq M_{\gamma_{EC}-\gamma_{EC}} \leq 0.17 \text{ GeV}$.



IC-IC

EC-EC

P_b measured using Moller Scattering



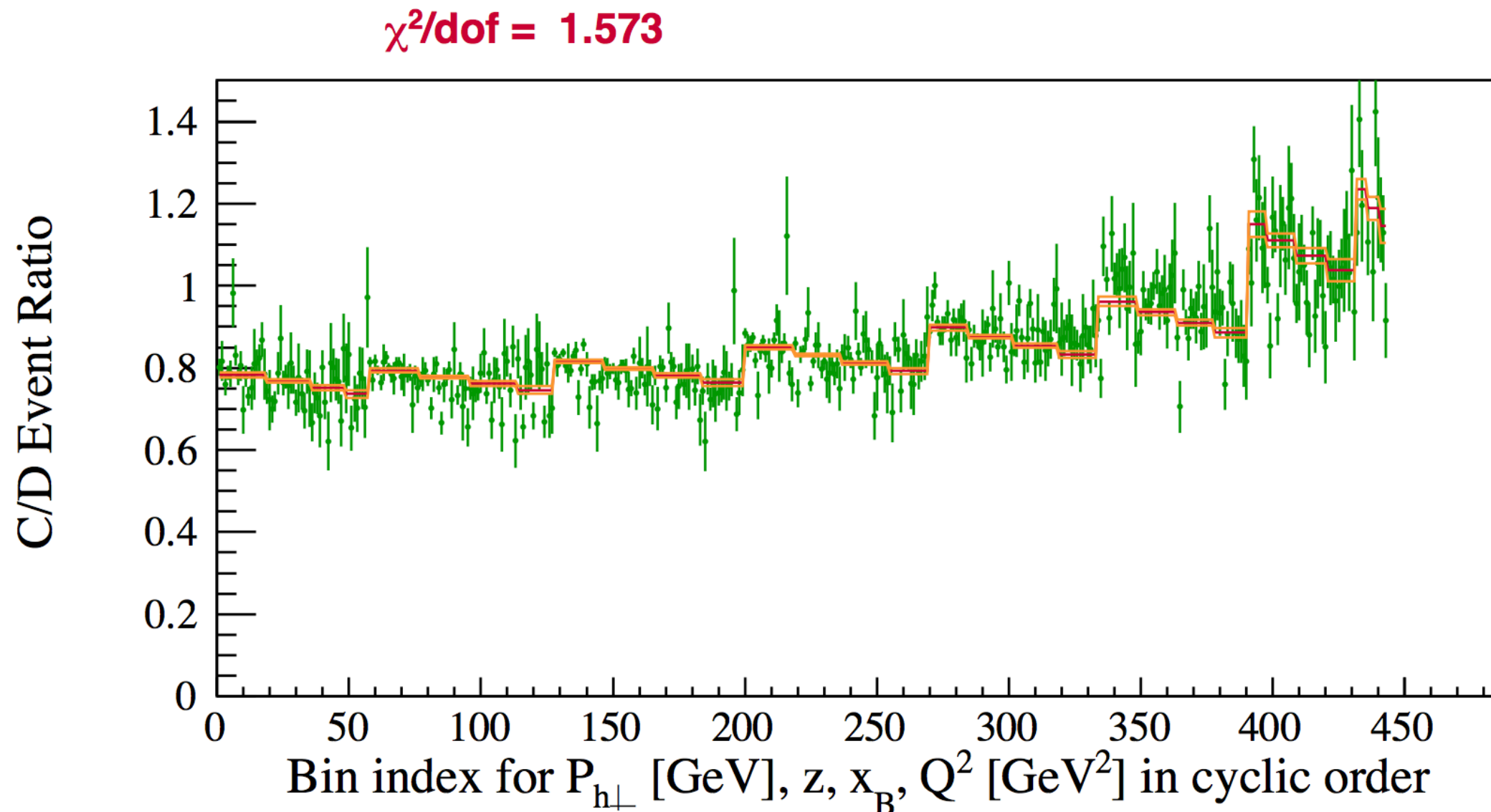


Figure 4.9: Fits of the ratio of neutral pion events on ^{12}C and ^2H from the EG2 experiment. Plotted along the x-axis are kinematic bins with $P_{h\perp}$ in the outer loop, then z , then x_B and Q^2 in the inner loop. The red line is the best fit; the two orange lines are the $\pm 1\sigma$ uncertainty of the fits. The ordering of the kinematic bin index in this figure is reverse of the following plots.



Complete lowest order radiative corrections to five-fold differential cross-section of hadron leptonproduction

I. Akushevich (Duke U.), A. Ilyichev (Minsk, High Energy Phys. Ctr.), M. Osipenko (INFN, Genoa & SINP, Moscow). Nov 2007. 15 pp.

Published in **Phys.Lett. B672 (2009) 35-44**

DOI: [10.1016/j.physletb.2008.12.058](https://doi.org/10.1016/j.physletb.2008.12.058)

Radiative effects in the processes of exclusive photon electroproduction from polarized protons

Igor Akushevich (Duke U. & Jefferson Lab), Alexander Ilyichev (Fermilab & Minsk, High Energy Phys. Ctr.). Jan 2012. 11 pp.

Published in **Phys.Rev. D85 (2012) 053008**

JLAB-PHY-11-1475

DOI: [10.1103/PhysRevD.85.053008](https://doi.org/10.1103/PhysRevD.85.053008)

CLAS Collaboration (P.E. Bosted (William-Mary Coll.) *et al.*). Nov 15, 2016. 12 pp.

Published in **Phys.Rev. C95 (2017) no.3, 035207**

JLAB-PHY-16-2388

DOI: [10.1103/PhysRevC.95.035207](https://doi.org/10.1103/PhysRevC.95.035207)

CLAS Collaboration (P.E. Bosted (William-Mary Coll.) *et al.*). Jul 25, 2016. 12 pp.

Published in **Phys.Rev. C95 (2017) no.3, 035206**

JLAB-PHY-16-2294

DOI: [10.1103/PhysRevC.95.035206](https://doi.org/10.1103/PhysRevC.95.035206)

CLAS Collaboration (P.E. Bosted (William-Mary Coll.) *et al.*). Apr 15, 2016. 25 pp.

Published in **Phys.Rev. C94 (2016) no.5, 055201**

JLAB-PHY-16-2294

DOI: [10.1103/PhysRevC.94.055201](https://doi.org/10.1103/PhysRevC.94.055201)

SIDIS radiative corrections are dominated by exclusive processes that radiate into the deep-inelastic region

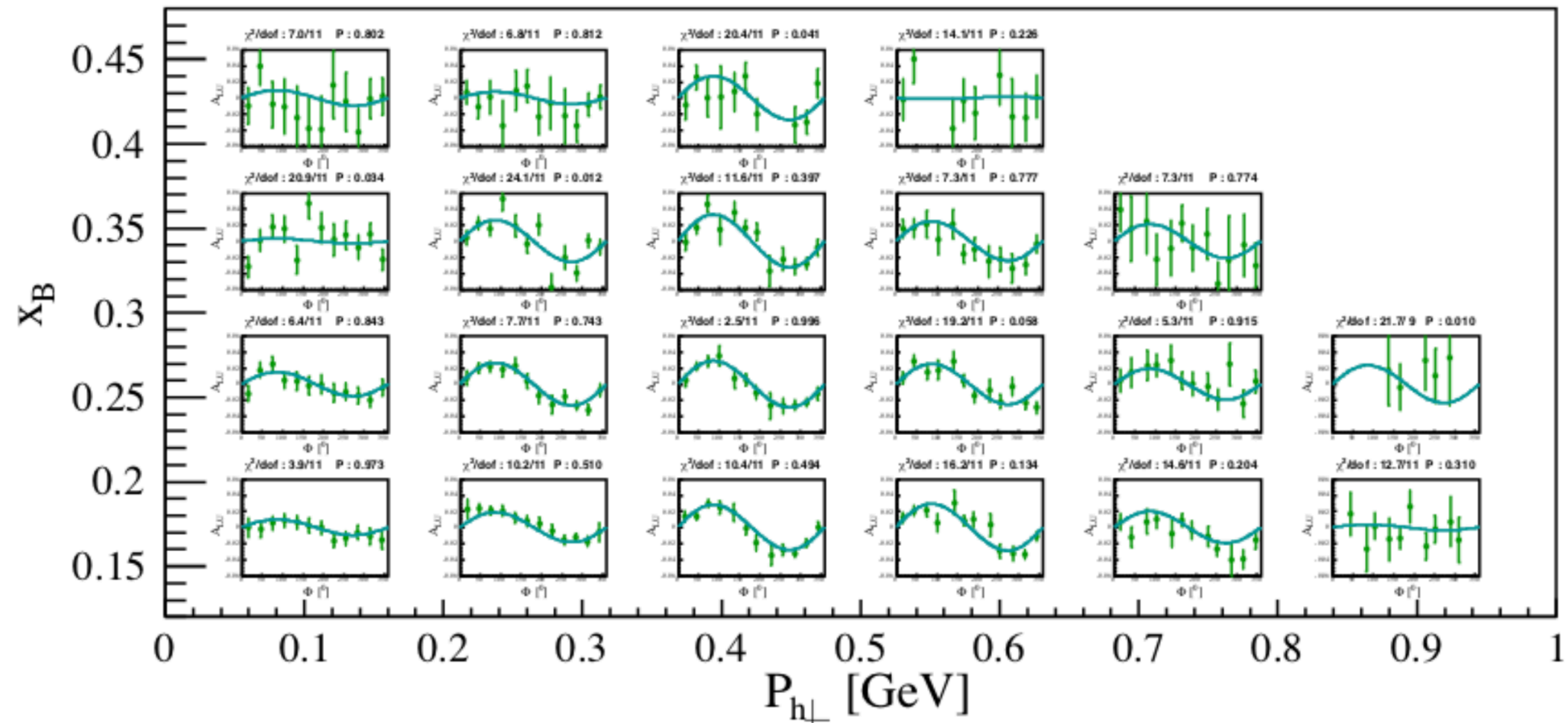


Figure 5.6: $A_{LU}(x_B, P_{h\perp}, \phi_h)$ on the proton for π^0

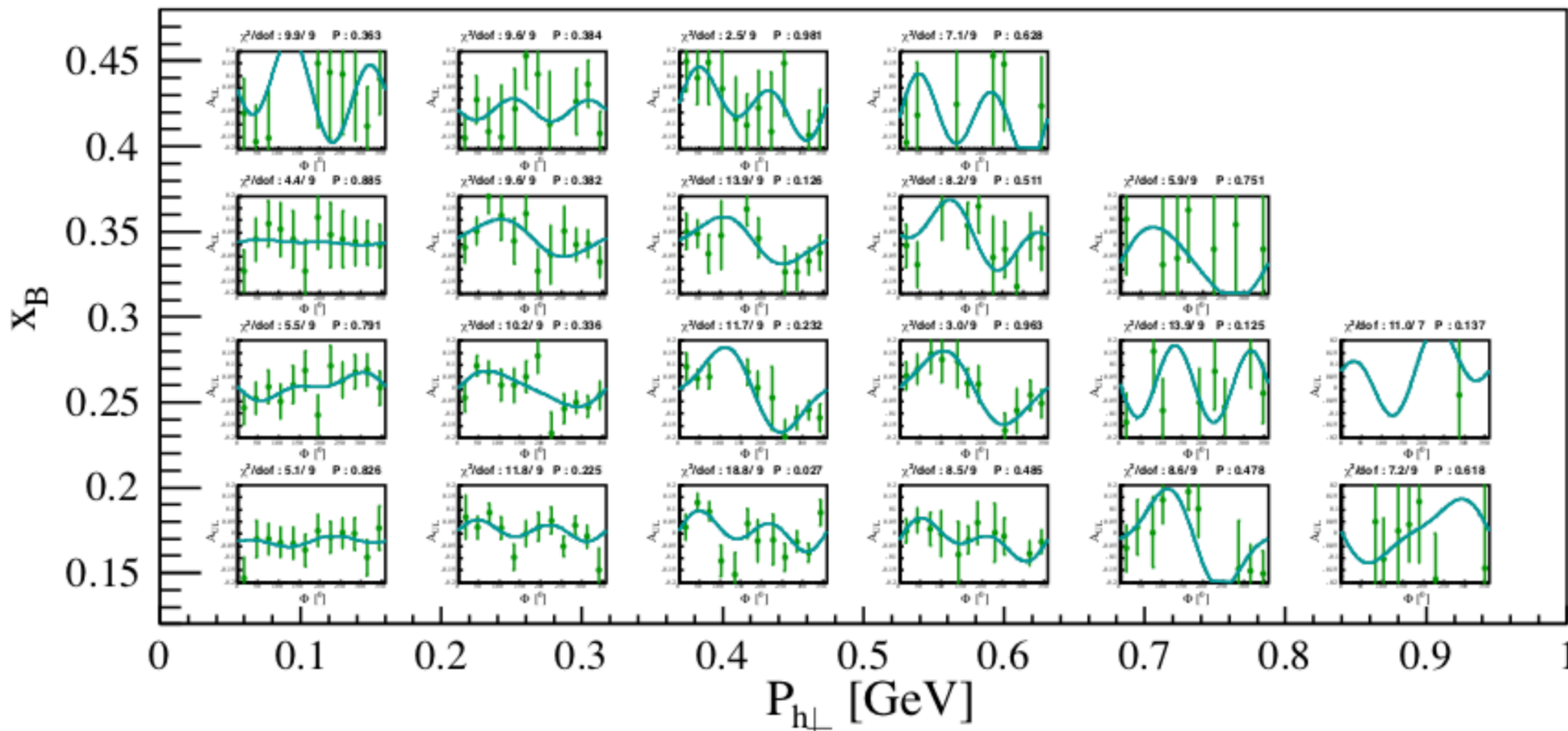


Figure 5.7: $A_{UL}(x_B, P_{h\perp}, \phi_h)$ on the proton for π^0

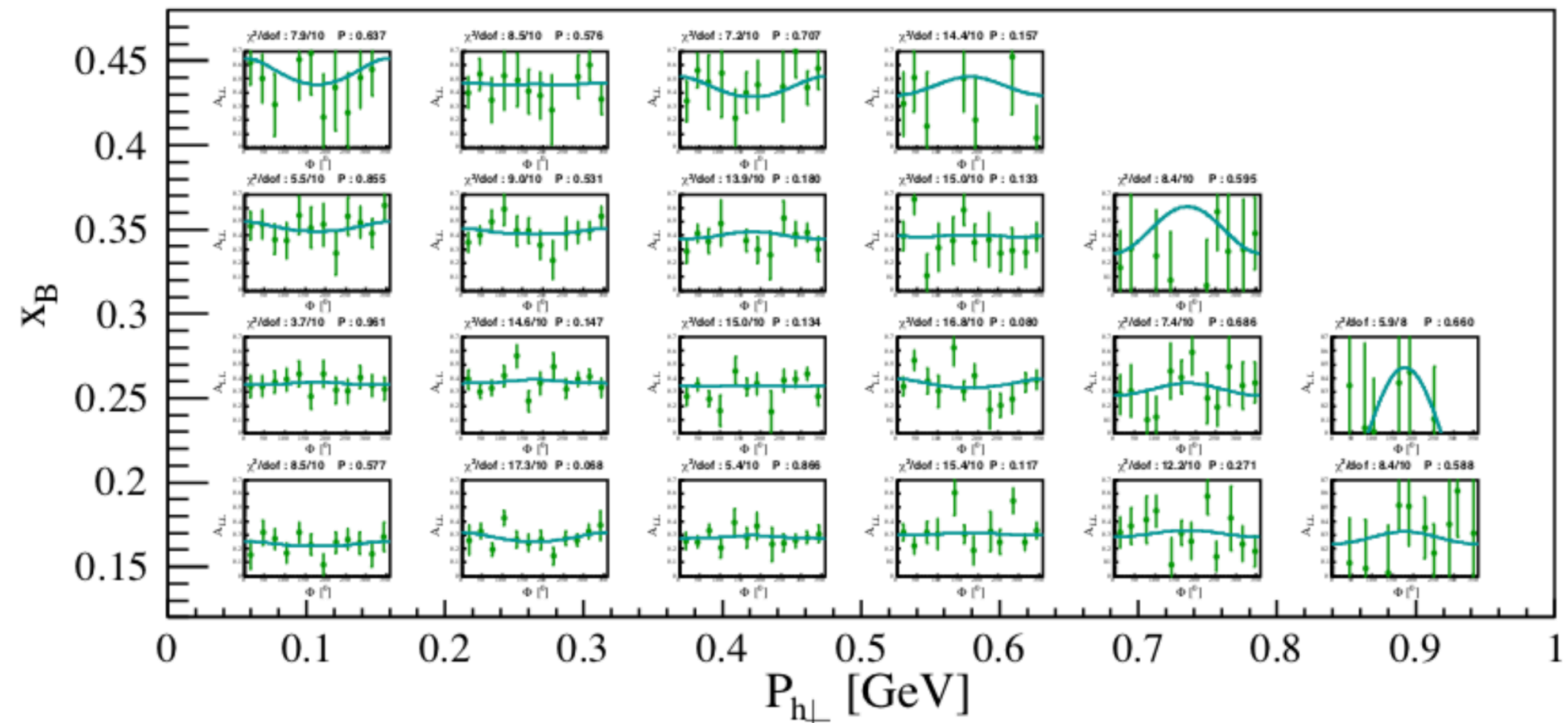


Figure 5.8: $A_{LL}(x_B, P_{h\perp}, \phi_h)$ on the proton for π^0

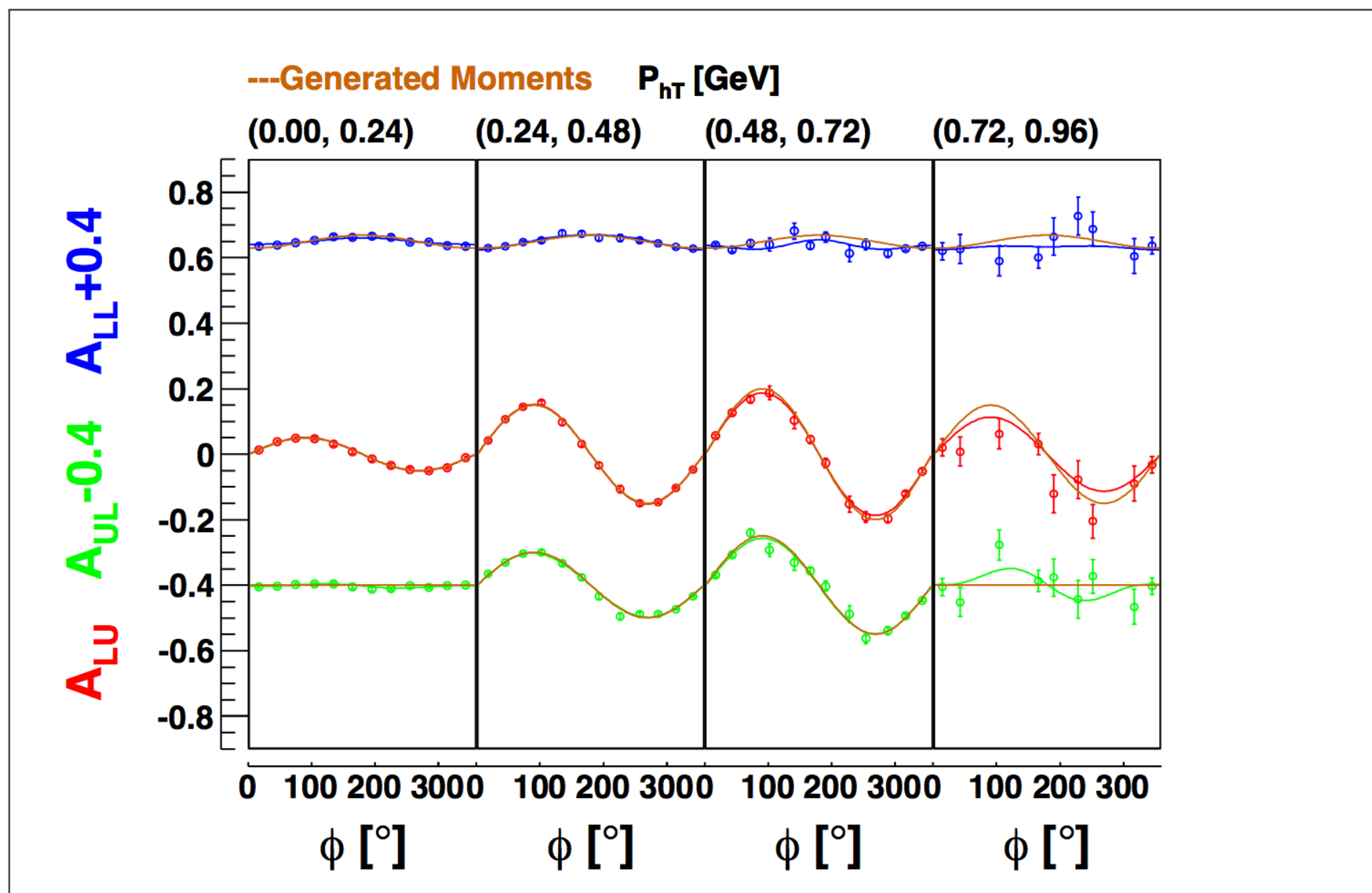


Figure 5.21: Comparison of generated and reconstructed asymmetries as a function of $P_{h\perp}$ for neutral pions.

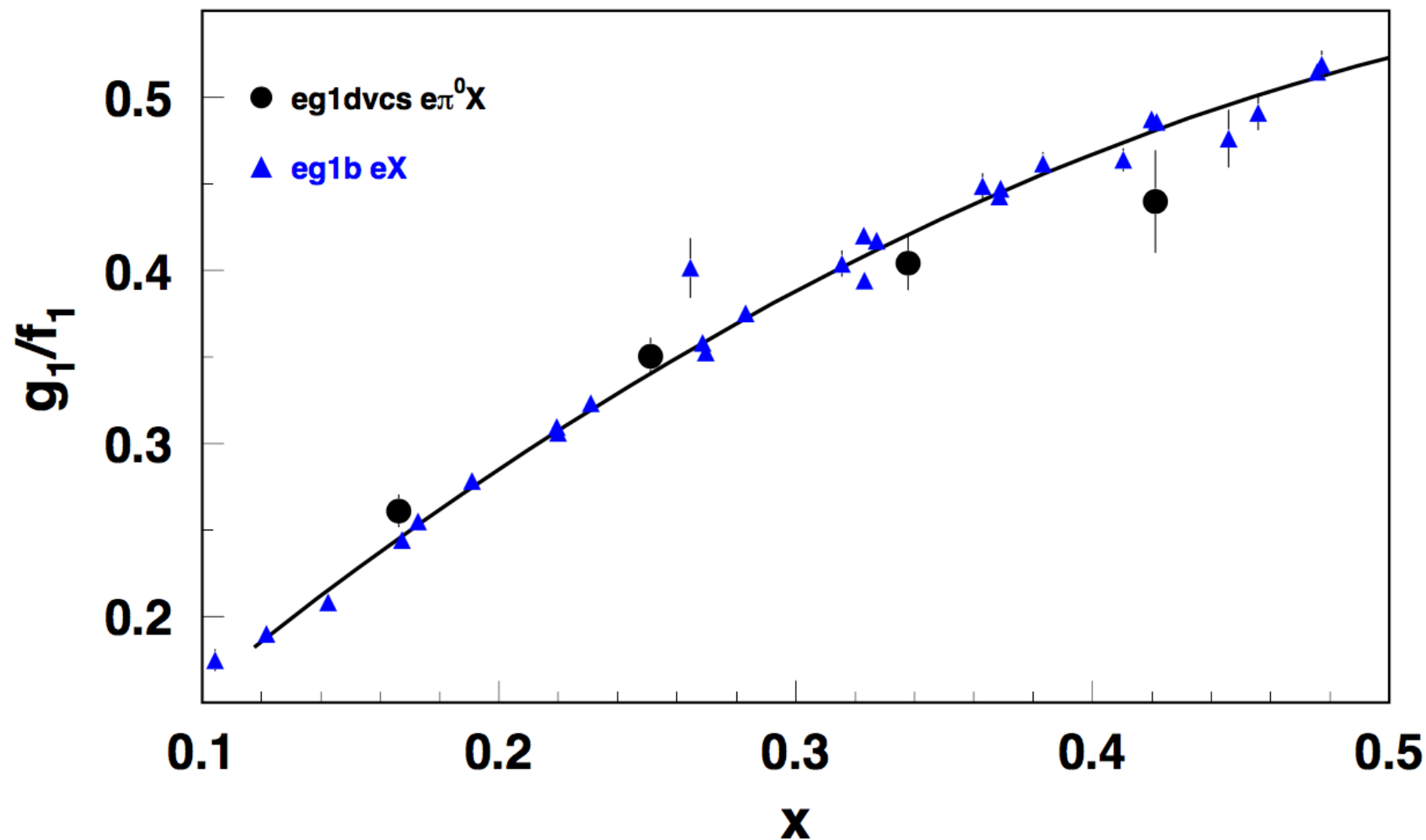
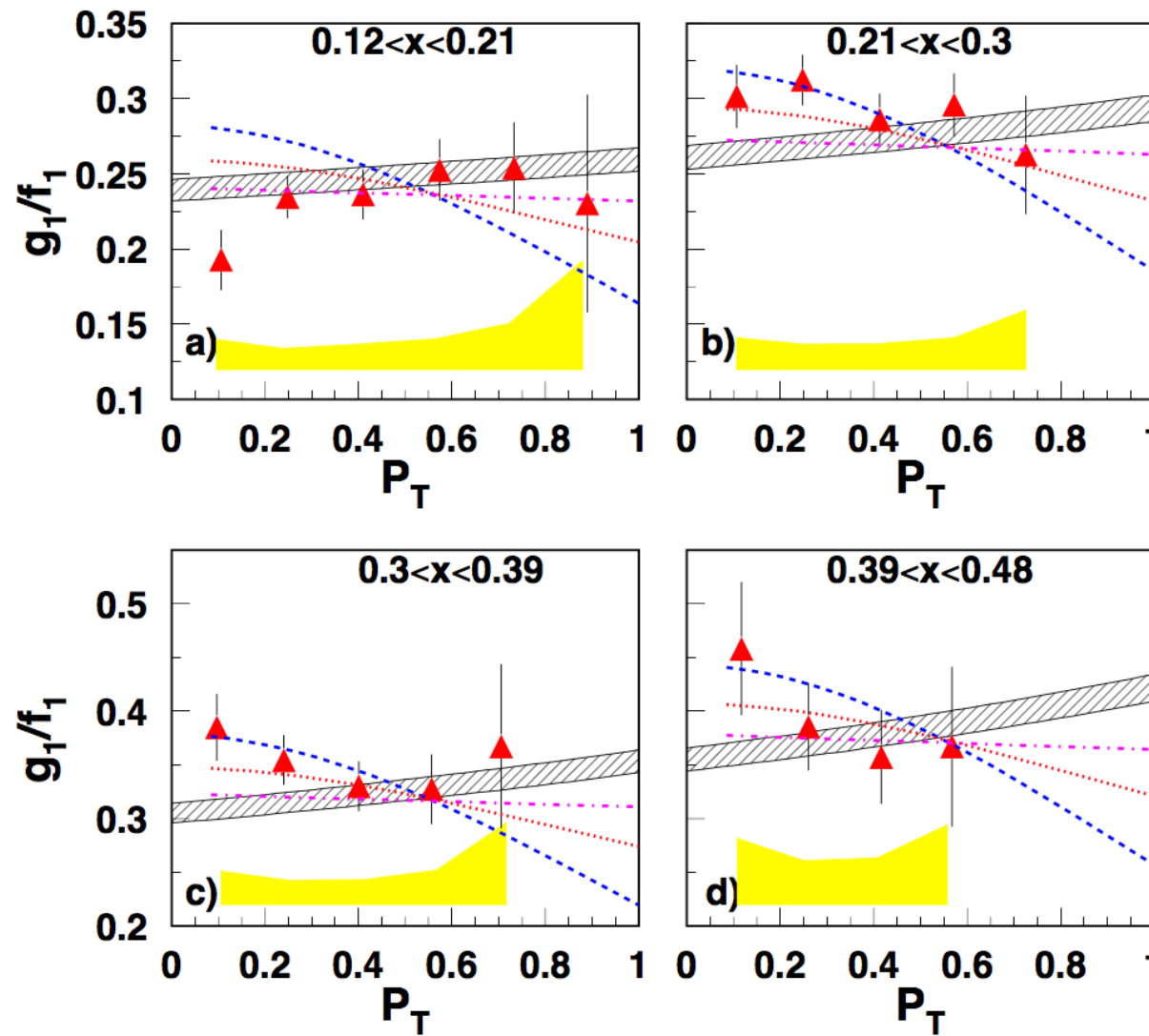


FIG. 1. g_1/f_1 versus x for π^0 compared with CLAS inclusive measurements [33]. The depolarization factor (Eq. 2 from Ref. [16]) has been calculated assuming $R = 0.1$ for the ratio of longitudinal to transverse photon cross sections.



- [41] C. Bourrely, J. Soffer, and F. Buccella, *Mod. Phys. Lett.* **A21**, 143 (2006), arXiv:hep-ph/0507328 [hep-ph].
- [42] C. Bourrely and J. Soffer, *Nucl. Phys.* **A941**, 307 (2015), arXiv:1502.02517 [hep-ph].

- [44] M. Anselmino, A. Efremov, A. Kotzinian, and B. Parsamyan, *Phys. Rev.* **D74**, 074015 (2006), arXiv:hep-ph/0608048 [hep-ph].

FIG. 2. The ratio g_1/f_1 versus P_T for π^0 DSAs, compared with calculations using the quantum statistical approach to parton distributions [41, 42] (gray bands). The dashed, dotted, and dash-dotted curves are calculations assuming that the g_1 to f_1 transverse momentum width ratios are 0.40, 0.68, and 1.0, respectively, using a fixed width for f_1 (0.25 GeV^2) [44]. The yellow bands are experimental total systematic errors.

Collins fragmentation function $H_{1\perp}$ is large and has opposite sign for the favored and unfavored cases. This suggests a significant suppression of the Collins fragmentation function for π^0

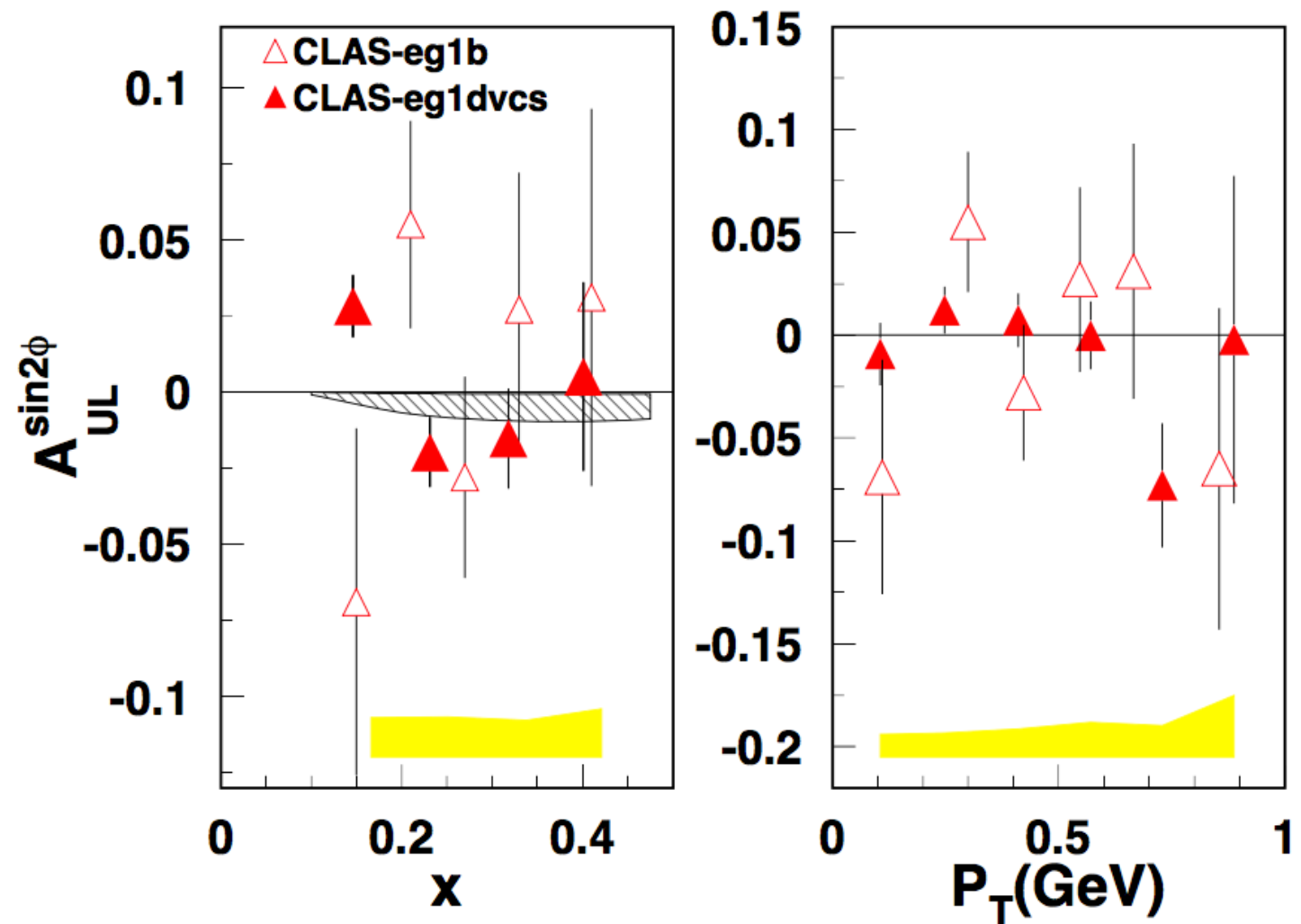
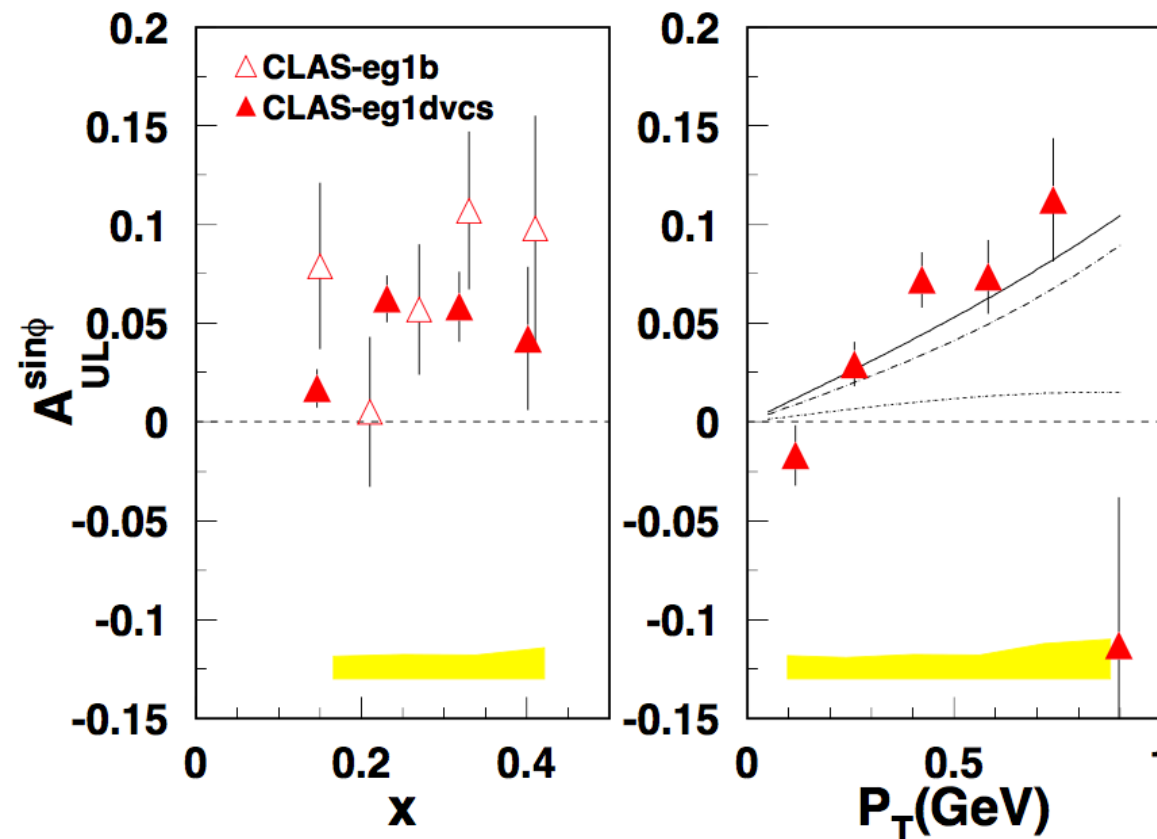


FIG. 3. $\sin 2\phi_h$ moments for A_{UL} plotted versus x (left) and P_T (right) compared to previous CLAS measurements [16] (which had limited π^0 kinematics) and theory predictions (gray band) [41, 42]. The yellow bands are experimental total systematic errors.

- [41] C. Bourrely, J. Soffer, and F. Buccella, Mod. Phys. Lett. **A21**, 143 (2006), arXiv:hep-ph/0507328 [hep-ph].
- [42] C. Bourrely and J. Soffer, Nucl. Phys. **A941**, 307 (2015), arXiv:1502.02517 [hep-ph].



- Data suggest that a Sivers-type contribution coming from the convolution of f_L^\perp and D1

FIG. 4. $\sin \phi_h$ moments for A_{UL} vs P_T . The open triangles are the old eg1b CLAS data [16] (which had limited π^0 acceptance), the and solid triangles are new measurements. The dashed and dotted lines are twist-3 calculations from Sivers (larger) and Collins (smaller) type terms [53, 54], respectively, and the solid line is the sum of the two. The yellow bands are experimental total systematic errors.

[53] W. Mao and Z. Lu, Phys. Rev. **D87**, 014012 (2013), arXiv:1210.4790 [hep-ph].

[54] Z. Lu and W. Mao, *Proceedings, 21st International Symposium on Spin Physics (SPIN 2014)*, Int. J. Mod. Phys. Conf. Ser. **40**, 1660045 (2016).

292 In summary, kinematic dependencies of single and dou-
293 ble spin asymmetries for neutral pions have been mea-
294 sured in multidimensional bins over a wide kinematic
295 range in x and P_T using CLAS with a polarized proton
296 target. Measurements of the P_T -dependence of the dou-
297 ble spin asymmetry, performed for the first time for dif-
298 ferent x -bins, indicate the possibility of different average
299 transverse momenta for quarks aligned or anti-aligned
300 with the nucleon spin. A non-zero $\sin \phi_h$ target single-
301 spin asymmetry was measured for neutral pions with high
302 precision, indicating that the target SSA may be gener-
303 ated through the Sivers mechanism. A small $\sin 2\phi_h$ mo-
304 ment of the target SSA is consistent with expectations of
305 strong suppression of the Collins effect for neutral pions,
306 due to cancellation of roughly equal favored and unfav-
307 ored Collins functions.



End



Ran February through September 2009

$^{14}\text{NH}_3$ and $^{14}\text{ND}_3$ Targets

80% and 30% polarizations, respectively

Expt. Part	Runs	Target	Vertex	Beam Energy	Torus Current
Part-A	58799 - 59155	NH_3	-58 cm	5.88 GeV	+2250 A
Part-B	59456 - 60184	NH_3	-68 cm	5.95 GeV	+2250 A
Part-C (a)	60304 - 60565	ND_3	-68 cm	5.75 GeV	+2250 A
Part-C (b)	60566 - 60648	ND_3	-68 cm	5.75 GeV	-2250 A